IEEE Access
Multidisciplinary | Rapid Review | Open Access Journal

SPECIAL SECTION ON NEURAL ENGINEERING INFORMATICS

Received January 17, 2019, accepted January 30, 2019, date of publication February 14, 2019, date of current version March 13, 2019.

Digital Object Identifier 10.1109/ACCESS.2019.2897908

A Complementary Method of PCC for the Construction of Scalp Resting-State EEG Connectome: Maximum Information Coefficient

YIN TIAN[1,2], HUILING ZHANG[1], PEIYANG LI[1], AND YANG LI[2]

[1]Bio-Information College, Chongqing University of Posts and Telecommunications, Chongqing 400065, China
[2]College of Computer Science and Technology, Chongqing University of Posts and Telecommunications, Chongqing 400065, China

Corresponding author: Yin Tian (tiany20032003@163.com)

This work was supported in part by the National Natural Science Foundation of China under Grant 61671097, and in part by the Chongqing Research Program of Basic Science and Frontier Technology under Grant cstc2017jcyjBX0007.

ABSTRACT Disclosing the complex relationships effectively between paired brain regions played a significant role in measuring the brain functional connectivity and exploring brain topological structures. Even though Pearson correlation coefficient (PCC) has been widely used to construct functional brain networks in the previous studies, it was mainly sensitive to linear associations. Therefore, maximal information coefficient (MIC) was first utilized to make up this weakness of PCC to construct electroencephalography (EEG) connectivity in the current study. The simulation results showed that MIC could capture certain relationships which PCC failed to detect. Furthermore, brain network properties changed with various thresholds under the resting-state EEG, and the comparison analysis of network properties illustrated that MIC and PCC could capture different aspects of connections between paired brain regions. These findings indicated that MIC could be a complementary method of PCC for the construction of scalp resting-state EEG connectome and provided a novel tool to reveal the potential mechanisms of brain networks.

INDEX TERMS EEG network, MIC, PCC, nonlinear, network properties.

I. INTRODUCTION

According to the principles of functional segregation and integration, human brain was one of the most complex systems in nature [1]. Diverse functional areas coordinated with each other to accomplish all kinds of cognitive processing, and associated with each other to form networks for carrying out specific functions. Recently, numerous studies have shown that the combination of the complex networks and the graph theory, i.e. connectome [2], could help to understand brain mechanisms [3], [4]. Therefore, it is utmost important to unlock the secrets of human brains in the network level.

Finding a proper method to define the edges of network played a key role. PCC was a well-established dependence measure and ranged from -1 (perfect but negative correlation) to $+1$ (total positive correlation) with 0 showing no correlation. It has been extensively applied to many fields such as quantifying colocalization [5], pattern recognition [6] and brain functional networks [7]. However, PCC was only sensitive to linear relationships, and its effectiveness greatly decreased when the dependence between paired nodes was nonlinear [8]. Moreover, PCC was not robust and seriously susceptible to outliers [9], [10]. In fact, any statistical metric based on sample averages like PCC could be affected by outliers inevitably [11]. In order to compensate for the shortcomings of this method, a mushrooming number of researchers turned their attention to find a novel way that was less vulnerable to the effects of outliers and more sensitive to capture both linear and/or nonlinear associations between two variables. Therefore, a variety of methods were put forward to quantify functional connections or networks, such as coherence based on magnetoencephalography (MEG) [12], [13] and EEG [14], [15], mutual information (MuI) using EEG data [16], distance correlation (Dcor) with functional magnetic resonance imaging (fMRI) [17] and MIC based on fMRI [18]. Using coherence in the distinct

The associate editor coordinating the review of this manuscript and approving it for publication was Peng Xu.

2169-3536 © 2019 IEEE. Translations and content mining are permitted for academic research only.
Personal use is also permitted, but republication/redistribution requires IEEE permission.
See http://www.ieee.org/publications_standards/publications/rights/index.html for more information.

groups, previous studies found that the sparse connectivity presented in the healthy groups, while the abundant connectivity and the obvious modular characteristics occurred in the epileptic patients [12]. However, owing to the complicated correlations between the active brain areas and the sensor recordings, it was difficult to obtain unambiguous information on the relevant brain areas, which hindered the derivation of any complex nonlinear associations by using coherence method [13]. Based on EEG, MuI, a method based on probability theory and/or information theory, quantified the amount of information obtained from one brain region to another, which could be applied to measuring both linear and nonlinear mutual associations [19], [20]. The limitation was that the calculation of probability distributions might be an obstacle for MuI [21]. Moreover, Dcor was proposed to identify functional network connectivity for exploring nonlinear dependence in rest-fMRI, which allowed both single-subject and group-level analyses [22]. In contrast to natural alternatives such as MuI and Dcor, MIC possessed two heuristic properties, namely generality and equitability [23]–[26], which could more equitably capture nonlinear correlations in high-dimensional data sets [23]. Additionally, the robust estimation of Shannon entropy and conditional entropy rendered MIC less susceptible to outliers [27], [28]. A recent study found that MIC outperformed other five common methods (i.e. CF, PCF, MuI, WCF and CH) in terms of consistency and robustness to capture brain functional connectivity from 75 healthy subjects in fMRI [20]. Moreover, based on MIC, Su *et al.* [29] successfully constructed non-linear functional connectivity and captured the non-linear properties of blood oxygenation level dependent (BOLD) signal. As mentioned above, MIC stood out from the crowd with high robustness and could also be used to define both linear and nonlinear dependence between paired variables [8]. However, MIC in previous studies was utilized to measure certain correlations based on fMRI which was mainly used for the detection of changes of local blood supply in the brain activated by specific stimuli [30], [31], but not based on EEG which recorded electrical activity of neural cells in the brain [32]. Moreover, MIC with its equitability properties gave similar scores to various types of relationships with the same noise level and provided a score for functional relationships with similar coefficient of determination when the sample size was large enough [23]. Thus, MIC could be used to reveal the variety of relationships in electrophysiological signals, such as EEG.

As a non-invasive technique, EEG could recorded signals from the surface of the skull [33], [34]. Moreover, due to its convenience, security and cheapness, EEG was widely utilized in various fields, such as feature extraction [35], classification [36], detection diagnosis of patients [37], [38]. Therefore, in the present study, EEG was applied in the establishment of functional brain networks.

Previous study evidenced that alpha activity could be found with eye opened and was maximal in the states of quiet restfulness [39]. Moreover, alpha frequency interactions reflected long-range integration during top-down processing [39] and could be used to detect changes of some mental diseases. For instance, progressive atrophy of hippocampus was correlated with the reduced cortical alpha power in mild cognitive impairment (MCI) and Alzheimer's disease (AD) [40]. Moreover, the decrease of alpha power was also correlated with visuospatial functions in obsessive-compulsive disorder (OCD) [41]. Therefore, alpha rhythm in resting state was utilized to construct brain functional networks in the current study.

In the current study, to reveal the complex relationships between two brain areas, MIC was utilized to construct the scalp resting-state EEG connectome. In addition, when estimating the effects of the connectivity measured by PCC and MIC, a suitable threshold should be selected to define the network edges. The network connections with weights equal or more than the given threshold could be retained, and otherwise the network edges are neglected [42], [43]. We attempted to find the differences on network properties (i.e. averaged path length, global efficiency, clustering coefficient, local efficiency, averaged node degree and small-world properties) based on two dependence measures (i.e. MIC and PCC) and tried to rationalize these discrepancies in the context of brain potential mechanisms. We hoped that these findings in the current study could be applied to validating the possible new brain connection measures and provided a reference for the exploration of functional EEG brain networks and topological structures.

II. MATERIALS AND METHODS

A. ETHICS STATEMENT

The experiment protocols were approved by the ethical committee of Chong Qing University of Posts and Telecommunications. Written informed consent was signed prior to participating in the experiment and subjects will receive monetary compensation after the experiment.

B. EEG RECORDINGS AND PRE-PROCESSING

Eighteen healthy and right-handed subjects (male: 9; Female: 9; mean age: 21 years old) participated in the experiment from the EEG Laboratory of Chongqing University of Posts and Telecommunications. None of them had mental or neurological problems. Each subjects' vision or corrected vision was normal. Subjects were required to sit in a comfortable chair and to focus on cross mark on the screen for 3 minutes. Subjects were expected to keep relaxed and stay awake as much as possible during the experiment. A 64-channel NeuroScan system was used for EEG data acquisition with a vertex reference. The EEG recordings were sampled at 1000 Hz and all EEG cap electrode impedances were kept below 5kΩ during the experiment.

In order to reduce the vertex reference electrode of influence on its surrounding electrodes, the data was offline re-referenced by the infinity reference (IR) [44], [45]. Electrooculogram (EOG) and Electromyography (EMG) were

excluded by Blind Source Separation (BSS) [46] and other noise was removed by automatic artifact rejection ($\pm 100\mu$v). EEG data was resampled at 250 Hz and EEG segments with 5s were chosen for the next network construction. And then the EEG recordings were filtered with a band-pass of 0.5-45Hz. To avoid the effect of volume conductor, 21 electrodes chosen by 10-20 system mapped the brain topology were selected as functional network nodes, i.e. Fp1, Fpz, Fp2, F7, F3, Fz, F4, F8, T7, C3, Cz, C4, T8, P7, P3, Pz. P4, P8, O1, Oz and O2. Then, MIC and PCC were utilized to capture the linear or nonlinear relationships among the power spectral density (PSD) of 21 electrodes under alpha rhythm. After that, according to the rules of threshold selection (see Threshold Selection section for details), suitable thresholds were selected to turn correlation matrices into binary matrices. In the binary matrices, there were only two values, that is, 0 and 1. 1 denoted the existing connection between two nodes and 0 indicated no connection between two nodes. Thus, whether there existed edge or connection between two nodes was measured by this way. Eventually, the rest-state functional networks were constructed successfully by two dependence measures (i.e. MIC and PCC). Moreover, the comparison of network properties for these two types of brain networks was analyzed to figure out whether MIC was a more suitable method to measure brain connectivity than PCC. Figure 1 displayed the overall workflow of brain network construction and analysis measured by MIC and PCC.

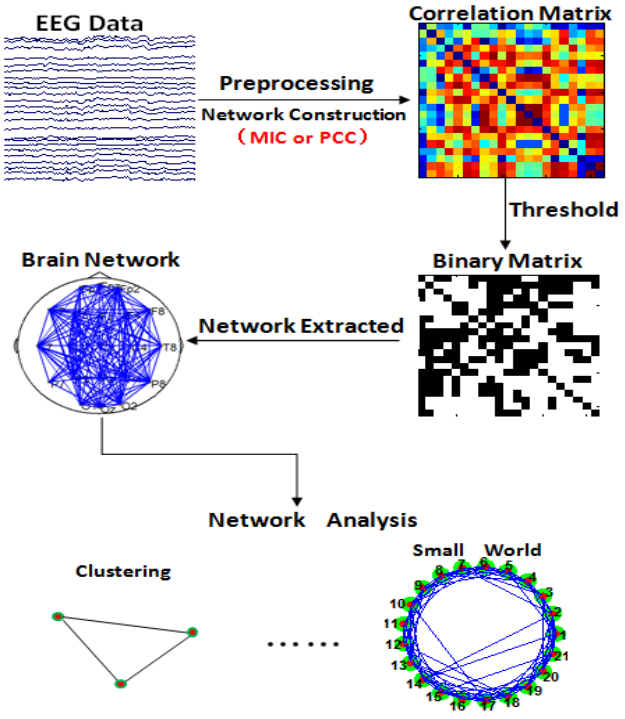

FIGURE 1. The construction processing of functional brain network.

C. PEARSON CORRELATION COEFFICIENT

PCC [47], [48] was widely used in measuring the linear correlation between two nodes x_i and y_i, and PCC was defined as

$$r = \frac{\sum_{i=1}^{n} (x_i - \bar{x})(y_i - \bar{y})}{\sqrt{\sum_{i=1}^{n} (x_i - \bar{x})^2}\sqrt{\sum_{i=1}^{n} (y_i - \bar{y})^2}} \quad (1)$$

in which was n denoted the length of variables; $\bar{x}$ and $\bar{y}$ represented the average of x and y, respectively. PCC ranged from -1 to 1, where 1 implied perfect positive correlation which could be described an absolutely linear relationship, 0 meant the absence of a relationship, and -1 denoted a total negative linear relationship. The closer the absolute value of PCC was to 1, the stronger the linear dependence between paired variables was.

D. MAXIMUM INFORMATION COEFFICIENT

MIC, proposed by Reshef *et al.* [24], was applied to measuring various (linear and nonlinear) dependence between two random variables a and b. The MIC could capture a wide range of relationships which were not only functional but also non-functional. The MIC (a, b) was defined as follows:

$$\begin{aligned} \mathrm{MIC}(a, b) &= \max\{\frac{I(a, b)}{\log_2 \min\{n_a, n_b\}}\} \\ &= \max\{\frac{H(a) + H(b) - H(a, b)}{\log_2 \min\{n_a, n_b\}}\} \end{aligned} \quad (2)$$

where $n_a \cdot n_b < B(n)$, $B(n) = n^{0.6}$. $H(a)$ and $H(b)$ were the marginal entropies, $H(a, b)$ was the joint entropy of variables a and b, and n_a and n_b were the sample size of variables a and b respectively. In theory, MIC ranged from 0 (weak correlation) to 1 (strong correlation), which gave scores similar with 1 for almost all kinds of noiseless functional relationships, and assigned scores approximate to 0 if the relationship between variables $a$and b were independent. In addition, owing to the symmetry of the mutual information I(a, b), MIC(a, b) was likewise symmetric, namely MIC(a, b) = MIC(b, a) [26]. In the current study, two types of scalp EEG correlation matrices were generated by MIC and PCC among electrodes pairs.

E. CORRELATION MATRIX AND FUNCTIONAL NETWORK CONSTRUCTION

Any networks were made up of nodes and edges between the paired nodes. In the current study, network nodes were specified as 21 EEG electrodes and edges were defined as the correlations (measured by MIC and PCC) between paired electrodes' PSD under alpha rhythm. That is, the computed PCC or MIC values were considered to be a symbol of the functional connectivity between two nodes of brain networks. For each subject, the correlations between all paired nodes were computed to obtain two types of 21 $\times$ 21 symmetric correlation matrices using MIC and PCC. Then, thresholds were used to transform the resulting correlation matrices into undirected binary graphs (networks), which also known as

adjacency matrices with 1 denoting strong correlation and 0 representing weak or no correlation.

In the present study, the binary graph (network) was constructed by applying a threshold T to PCC or MIC. And the specific steps were as follows:

$$e_{ij} = \begin{cases} 1, & if \ |r_{ij}| \geq T \\ 0, & otherwise \end{cases} \tag{3}$$

where e_{ij} denoted the edge in the binary network. If the elements of adjacency matrix r_{ij} (i.e. network connection value) larger than (or equal to) the given threshold T would be set to 1, the edges were assumed to exist; otherwise the edges did not exist [49].

F. THRESHOLD VALUE SELECTION

Selecting a threshold was a flexible and crucial step when establishing functional networks, because network characteristics were closely related to the choice of thresholds. Since there was no explicit standard for threshold selection in the state of the art, here we selected a range of thresholds to study the topological properties of brain networks [50]. Thresholds were chosen to exclude the weak correlation (regarded as noise), and meanwhile to guarantee network connectivity (i.e., no isolated nodes). In the present study, the threshold range was selected to meet two rules. One was that the constructed networks were required to satisfy small-world properties, namely $\sigma > 1$, $\gamma > 1$ and $\lambda \approx 1 (p < 0.05$, FDR corrected) [1]; the other was that the averaged node degree of networks (Deg) was required to be not less than $2\ln N$ (N denoted the number of network nodes), i.e., $Deg \geq 2\ln(21)$, to ensure the networks to meet the connectivity of the nodes [10], [42].

G. NETWORK CHARACTERISTIC METRICS

With regard to the brain networks, the averaged path length of the network (Lp), the global efficient (Eg), the clustering coefficient (CC), the local efficient ($Eloc$), the averaged node degree (Deg) and small-world network properties were usually calculated to analyze brain functional network characteristics [10].

1) AVERAGE PATH LENGTH

The shortest path length specified the optimal path of information transfer from one node (i.e. electrode or brain region) to another in the functional networks [51]. Information could be delivered more quickly and efficiently through the shortest path length. The shortest path length L_{ab} between two nodes a and b was the access with the least number edges. The averaged path length of network (Lp) of networks denoted the mean of the shortest path length for all nodes, which could be defined as:

$$Lp = \frac{1}{N(N-1)} \sum_{a,b \in V, a \neq b} L_{ab} \tag{4}$$

where V was the collection of all nodes in the networks (i.e., functional brain networks), and n was the number of nodes. the smaller Lp indicated the higher information transfer efficiency.

2) GLOBAL EFFICIENCY

Global efficiency (Eg) was the extension of averaged path length of networks and could measure the global transmission ability of networks [43]. For a network V with N nodes, the Eg of V could be calculated as:

$$Eg = \frac{1}{N(N-1)} \sum_{a,b \in V, a \neq b} \frac{1}{L_{ab}} \tag{5}$$

The shorter the value of Lp was, the bigger Eg was and the stronger the capability of global information propagation of the network was.

3) CLUSTERING COEFFICIENT

Clustering coefficient of a node, C_a, described the level of connectedness of the direct neighbors of the node [50] and was a measure of the extent of network collectivization. C_a was calculated as the ratio of the number of actually existing connections divided by the maximum possible number of connections in the subgraph V_a:

$$C_a = \frac{2e_a}{k_a(k_a - 1)} \tag{6}$$

where e_a was the number of actually existing edges in the subgraph V_a.

The clustering coefficient of networks, C_{net}, was the mean of the clustering coefficient of all nodes:

$$C_{net} = \frac{1}{N} \sum_{a \in V} C_a \tag{7}$$

4) LOCAL EFFICIENCY

The local efficiency of subgraph V_a was computed as the average of the shortest path of all nodes in the subgraph V_a [43].

$$Eloc_a = \frac{1}{N_{V_a}(N_{V_a} - 1)} \sum_{b,c \in V_a, c \neq b} \frac{1}{L_{bc}} \tag{8}$$

where L_{bc} was the shortest path between node b and c in the subgraph V_a. $Eloc_a$ indicated the ability of information exchange after removing node a in the subgraph V_a. The local efficiency of a network could be specified as:

$$Eloc_{net} = \frac{1}{N} \sum_{a \in V} Eloc_a \tag{9}$$

$Eloc_{net}$ could depict the local information transmission ability of the network [43].

5) AVERAGED NODE DEGREE

Within undirected graph, Deg_a, i.e. the degree of node a, was regarded as the number of nodes directly connected with node a. One node with higher degree had more connections [1] and played a more indispensable role in the network.

The average node degree of networks was measured as the mean of the degrees of all the nodes:

$$Deg = \frac{1}{N}\sum_{a\in V} Deg_a \tag{10}$$

Deg represented the sparsity of networks.

6) SMALL WORLD PROPERTIES

Relative to random networks, small world networks held higher clustering coefficient and similar averaged path length [52], namely:

$$\begin{aligned}\gamma &= Cp^{real}/Cp^{random} > 1\\ \lambda &= Lp^{real}/Lp^{random} \approx 1\end{aligned} \tag{11}$$

where Cp^{real} and Cp^{random} denoted the clustering coefficient of the real networks and random networks respectively, while Lp^{real} and Lp^{random} represented the averaged path length of the real and random networks, respectively.

Combining two small world indices γ and λ, a scalar quantitative measurement, σ, could be utilized to examine 'small-world-ness' of networks easily [53]. That is:

$$\sigma = \gamma/\lambda \tag{12}$$

when σ was significantly greater than 1, we considered that the networks satisfied small world properties. In the current study, Malslovs wring algorithm was used to generate random networks with the same number of nodes, number of edges and degree distributions as real binary networks [49], [54].

H. SIMULATION

In order to validate the possible new connection measures for EEG brain network, three simulated models were did in the current study. For the current simulated network with three nodes, the relationships between nodes were mutually influential. If we determined the functional relationships (linear or nonlinear) of two edges in a 3-node network, then the third edge could be derived from the previously determined functional relationships of the other two edges.

1) SIMULATED MODEL 1

Model 1 was a 3-node network with full linear correlations. For Model 1, we firstly made sure that the functional relationships $f_{A,B}$ and $f_{C,B}$ were linear relationships. That is, $f_{A,B}$ and $f_{C,B}$ satisfied superposition principle (i.e. $f(x+y) = f(x)+f(y)$) and homogeneity (i.e. $f(ax) = af(x)$, a was the constant coefficient). $f_{A,B}$ denoted the functional relationship between node A and B. Similarly, $f_{C,B}$ denoted the functional relationship between node C and B. Then, the functional relationship between node A and C (i.e. $f_{A,C}$) could be derived by $f_{A,B}$ and $f_{C,B}$.

Within the Model 1, functional relationships among the three nodes were as follows:

$$x_A = 4x_B + \varepsilon \tag{13}$$

$$x_C = 4x_B + \varepsilon \tag{14}$$

$$x_C = x_A + \varepsilon \tag{15}$$

where x_A, x_B and x_C were the values of three nodes in the simulated network and all subjected to the normal distribution, namely $x_A, x_B, x_C \sim$ N(0,1). ε was noise and subjected to the uniform distribution, namely $\varepsilon \sim$ U(0,1).

2) SIMULATED MODEL 2

Model 2 was a 3-node network with two nonlinear correlations and one linear correlation. Similar with Model 1, we firstly ensured that $f_{A,B}$ was linear and $f_{C,B}$ was nonlinear. Then, the functional relationship between node A and C (i.e. $f_{A,C}$) could be derived by $f_{A,B}$ and $f_{C,B}$. Within the Model 2, functional relationships among the three nodes were as follows:

$$x_A = 4x_B + \varepsilon \tag{16}$$

$$x_C = 4\sin x_B + 3x_B^2 + \varepsilon \tag{17}$$

$$x_C = 4\sin(\frac{1}{4}x_A) + \frac{3}{16}x_A^2 + \varepsilon \tag{18}$$

where x_A, x_B and x_C were the values of three nodes in the simulated network and all subjected to the normal distribution, namely $x_A, x_B, x_C \sim$ N(0,1). ε was noise and subjected to the uniform distribution, namely $\varepsilon \sim$ U(0,1).

3) SIMULATED MODEL 3

Model 3 was a 3-node network with full nonlinear correlations. Firstly, we made sure that the functional relationships $f_{A,B}$ and $f_{C,B}$ were nonlinear. Then, the functional relationship $f_{A,C}$ could be derived by $f_{A,B}$ and $f_{C,B}$. Within the Model 3, functional relationships among the three nodes were as follows:

$$x_A = x_B^2 + \varepsilon \tag{19}$$

$$x_C = 4\sin(x_B^2) + 3x_B^2 + \varepsilon \tag{20}$$

$$x_C = 4\sin(x_A) + 3x_A + \varepsilon \tag{21}$$

where x_A, x_B and x_C were the values of three nodes in the simulated network and all subjected to the normal distribution, namely $x_A, x_B, x_C \sim$ N(0,1). ε was noise and subjected to the uniform distribution, namely $\varepsilon \sim$ U(0,1).

III. RESULTS

A. SIMULATION STUDY

For three simulated networks, the correlations among three nodes were measured by PCC and MIC. The simulated results were showed in TABLE 1 $\sim$ TABLE 3. Within Model 1, the PCC and MIC between node A and B were 0.643 and 0.775 ($p < 0.05$) respectively. The PCC and MIC between

TABLE 1. Simulated model 1.

Model 1	$x_A \sim x_B$	$x_C \sim x_B$	$x_A \sim x_C$
PCC	0.643*	0.760*	0.564**
MIC	0.775*	0.748*	0.786**

Notes: * denoted $p < 0.05$; ** denoted $p < 0.001$.

TABLE 2. Simulated model 2.

Model 1	$x_A \sim x_B$	$x_C \sim x_B$	$x_A \sim x_C$
PCC	0.594*	0.769*	0.392
MIC	0.673*	0.894*	0.729*

TABLE 3. Simulated model 3.

Model 1	$x_A \sim x_B$	$x_C \sim x_B$	$x_A \sim x_C$
PCC	0.439	0.312	0.942**
MIC	0.627*	0.633*	0.967**

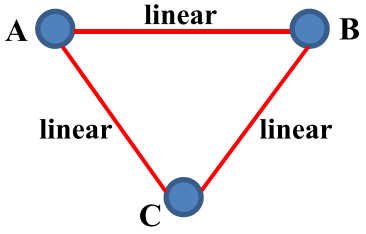

FIGURE 2. Model 1: simulated network with linear edges. A, B and C denoted the three network nodes.

node *C* and *B* were 0.760 and 0.748 ($p < 0.05$), respectively. The PCC and MIC between node *A* and *C* were 0.564 and 0.786 ($p < 0.001$), respectively. Within Model 2, the PCC and MIC between node *A* and *B* were 0.594 and 0.673 ($p < 0.05$), respectively. The PCC and MIC between node *C* and *B* were 0.769 and 0.894 ($p < 0.05$), respectively. The PCC and MIC between node *A* and *C* were 0.392 ($p > 0.05$) and 0.729 ($p < 0.05$), respectively. Within Model 3, the PCC and MIC between node *A* and *B* were 0.439 ($p > 0.05$) and 0.629 ($p < 0.05$), respectively. The PCC and MIC between node *C* and *B* were 0.312 ($p > 0.05$) and 0.633 ($p < 0.05$), respectively. The PCC and MIC between node *A* and *C* were 0.942 and 0.967 ($p < 0.001$), respectively.

B. NETWORK PROPERTY ANALYSIS

As the Figure 5 illustrated that the minimum was set to 0.5 for removing weak or false connections and at the same time ensuring the small-worldness of alpha networks, namely σ and γ significantly greater than 1 ($p < 0.05$, FDR corrected), and λ was approximately equal to 1 ($p > 0.05$). The maximum threshold was 0.73 to ensure that the *Deg* of alpha networks exceeds 6.08 (i.e. 2ln21) for meeting the connectivity between nodes. Hence here the threshold range was in 0.5∼0.73 (with steps of 0.01).

In the current study, we did the statistical analysis for the structure of EEG networks (i.e. network properties). At each threshold point, the paired t-test was performed to examine whether there was a significant difference between network properties established by MIC and PCC. The blue star ($\star$) denoted that there was a significant difference on network properties between MIC- and PCC-based networks ($p < 0.05$, FDR corrected).

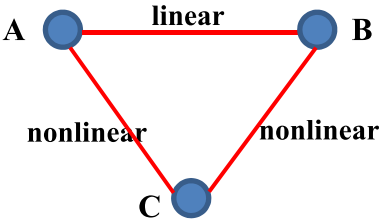

FIGURE 3. Model 2: simulated network with linear and nonlinear edges. A, B and C denoted the three network nodes.

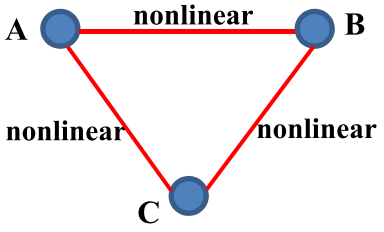

FIGURE 4. Model 3: simulated network with nonlinear edges. A, B and C denoted the three network nodes.

As Figure 5 (A) illustrated, alpha networks measured by MIC and PCC both satisfied small-word properties. As showed in Figure 5 (B), *Cp*, *Lp*, *Eloc*, *Eg* and *Deg* of the constructed network by MIC overmatched the *Cp* of the constructed network by PCC when the thresholds respectively was in 0.5∼0.52, 0.5∼0.6 (or 0.68∼0.73), 0.5∼0.54, 0.5∼0.6 (or 0.65∼0.72) and 0.5∼0.59, while the *Cp* and *Eloc* of the network obtained from MIC was inferior to that obtained from PCC markedly when the threshold ranges were in 0.55∼0.61 (or 0.64∼0.73) and 0.64∼0.73.

IV. DISCUSSION

In the current study, we investigated the topological differences between two types of networks measured by MIC and PCC and tested the effects of connectivity characteristics within a given threshold range. From the simulation and the resting-state brain network results, we found that: (1) Compared to MIC, PCC was more widely used and easier to implement. However, from the simulation study, PCC could not accurately capture nonlinear relationships between two nodes of simulated networks, which indicated that MIC could be a complementary method of PCC to measure the relationship between two nodes. (2) As showed by the network properties analysis from the real EEG data, for the edge number of the constructed network measured by both MIC and PCC, the network connectivity was sparser with the increased thresholds and conversely, network density grew with the decreased thresholds. (3) On the whole, the brain network properties measured by MIC was superior to those measured by PCC, which indicated that MIC could capture a variety of potentially interesting relationships between paired brain regions which PCC failed to capture. However, the *Cp* and *Eloc* of EEG networks measured by MIC was inferior to those measure by PCC in higher threshold ranges, which implied

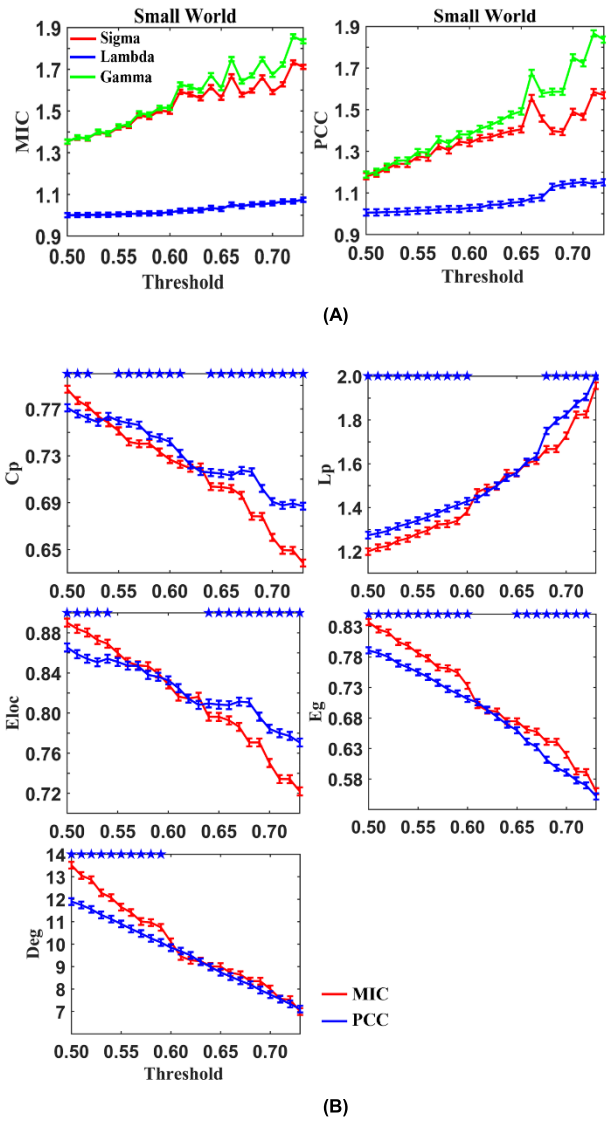

FIGURE 5. Properties of alpha networks constructed by MIC and PCC. (A) Small world properties of networks varied with different thresholds. (B) *Cp*, *Lp*, *Eloc*, *Eg* and *Deg* changed with different thresholds. The red color showed the properties of brain networks estimated by MIC, and the blue color represented the properties of brain networks computed by PCC. The vertical axes denoted the network properties, and the horizontal axes indicated step-by-step thresholds (step: 0.01). The blue star (⋆) suggested that there was a significant difference between network properties established by MIC and PCC ($p < 0.05$, FDR corrected).

that MIC and PCC could capture different parts of relationships between two brain areas. That is, the combination of PCC and MIC might reveal deeper topology of functional brain networks. Here, MIC was firstly applied to measuring the functional connections for EEG networks, which might provide a novel method for EEG brain connectome.

As showed by simulation study, both PCC and MIC could capture linear relationships in simulated model 1. However, PCC could not exactly measure the nonlinear relationships between node *A* and node *C* in simulated model 2. In addition, not only the nonlinearity between node *A* and node *B*, but also the nonlinearity between node *C* and node *B* could not properly be represented by PCC in simulated model 3. Moreover, the nonlinearity between node *A* and node *C* in simulated model 3 could be mistakenly measured by PCC in a highly linearity-related pattern. The results implied that MIC could capture some nonlinear relationships between two variables and some complex disease associations, such as single-nucleotide polymorphism (SNP) disease [55] and germ cell tumors (GCT) [56], which PCC might have difficulty to measure.

Based on the EEG networks showed by Figure 5, as the thresholds increased, the *Cp*, *Eloc*, *Eg*, *Deg* of alpha networks decreased and the *Lp* of alpha networks increased constructed by MIC and PCC which indicated that information transmission ability of networks declined and the network connectivity declined (sparser). Similarly, as the thresholds decreased, the *Cp*, *Eloc*, *Eg*, *Deg* of alpha networks increased and the *Lp* of alpha networks decreased, indicating that information transmission ability of the networks increased and the network connectivity increased (denser). Moreover, as Figure 5 showed, *Eloc*, *Eg* and *Deg* based on MIC, were mostly superior to those based on PCC in the lower threshold ranges, indicating that network density and capability for parallel information propagation of the construed networks by MIC was higher than that by PCC within lower thresholds. These findings suggested that MIC could be used to define more relationships (functional and non-functional relationships) between paired brain regions but lower degree of correlations (or weights of connectivity matrix) than PCC, which further embodied the generality properties of MIC, consistent with the previous studies [20], [24]. Enlightened by these findings above, we could come to a conclusion that with the changes of different cognitive processes such as working memory, emotion and attention, inter-regional interactions or integration were performed by varying linear or nonlinear relationships among neurons and neuronal assemblies which also played a critical role in the construction of network topology.

Our results indicated that alpha networks were organized in an efficient small-world manner that confirmed at high efficiency of information processing at relatively low connection cost. In other words, the features of alpha networks in the current study were high clustering coefficients and low path lengths [57].

In addition, the denser connection (i.e. node degree) and more global connectivity (i.e. long-distance interrelationship) in the lower threshold ranges occurred in alpha networks based on MIC to guarantee the efficient information processing and transfer of the inhibitory and excitation. This might indicate that nonlinear characteristics took the dominant position during area-to-area network interactions of alpha processing, consistence with the previous study [58]. In the higher threshold ranges, the alpha network showed relatively stable connections between distant brain areas based on MIC, while we found the local information transfer efficiency in the network constructed by PCC was significantly higher than that by MIC. Previous findings revealed that local alpha oscillation might negatively associated with the excitability

of cortical processing [59]. That is, the brain networks in the higher threshold ranges might showed more linear parts of the local and inter-areal alpha dynamic cortical interactions but not non-linear parts.

Taken together, the distinct brain network topology might reveal different varieties of dynamic processes of perception arousal level, excitation, inhibition, and motor-related activity, which might be reflected by the linear or nonlinear mode measured by PCC and MIC respectively.

MIC might be a proper dependence measure that could capture certain associations which PCC could not find. However, computational complexity of MIC was much greater than that of PCC. Although MIC was considered a great progress in dependence measures between two variables [8], there were still a lot of steps to take in the implementation for the dependence measure. Moreover, MIC as a nonlinear method cannot completely be regarded as a substitution for the linear method like PCC and nonlinear methods were not always more effective than linear methods [60]. Instead, nonlinear methods should be referred to as a complementary to linear methods. Different parts of dependence relationships between paired variables could be measured by the linear and nonlinear methods together. Therefore, seeking a proper method to capture associations between two variables deserved to be taken seriously based on the cognitive characteristics of the acquired data and the experimental motivation.

V. CONCLUSION

In the current study, firstly the correlations between two nodes of three simulated models were measured by MIC and PCC to validate the possible new connection measures for EEG brain networks. Secondly, MIC and PCC were respectively utilized to construct resting-state brain functional networks underlying high temporal resolution EEG recordings. Then, a threshold range was given to check the connectivity characteristics of constructed networks by both MIC and PCC.

More importantly, the results showed that MIC could capture certain associations which PCC failed to do. However, it might be a misconception that MIC could absolutely be a substitution for PCC. The comparison analysis of network properties underlying the resting-state EEG recordings indicated that MIC could not absolutely be a substitution for PCC, that is, MIC and PCC could capture different aspects of connections between two brain areas. In other words, the nonlinear method was not always more effective than the linear method. In effect, nonlinear methods were considered as a complementary approach to linear methods and different parts of associations between two variables could be found by the two kinds of methods collectively.

REFERENCES

[1] W. Liao *et al.*, "Altered functional connectivity and small-world in mesial temporal lobe epilepsy," *PLoS ONE*, vol. 5, no. 1, p. e8525, 2010.

[2] E. Bullmore and O. Sporns, "Complex brain networks: Graph theoretical analysis of structural and functional systems," *Nature Rev. Neurosci.*, vol. 10, no. 3, pp. 186–198, Mar. 2009.

[3] C. J. Stam and J. C. Reijneveld, "Graph theoretical analysis of complex networks in the brain," *Nonlinear Biomed. Phys.*, vol. 1, p. 3, Jul. 2007.

[4] J.-F. Sun, X.-F. Hong, and S.-B. Tong, "A survey of complex brain networks: Structure, function, computation, and applications," *Complex Syst. Complex. Sci.*, vol. 7, pp. 74–90, 2010.

[5] J. Adler and I. Parmryd, "Quantifying colocalization by correlation: The Pearson correlation coefficient is superior to the Mander's overlap coefficient," *Cytometry A*, vol. 77A, pp. 733–742, Aug. 2010.

[6] F. Coelho, A. P. Braga, and M. Verleysen, "Multi-objective semi-supervised feature selection and model selection based on Pearson's correlation coefficient," in *Proc. Prog. Pattern Recognit., Image Anal., Comput. Vis., Appl.-Iberoamerican Congr. Pattern Recognit. (CIARP)*, Sao Paulo, Brazil, Nov. 2010, pp. 509–516.

[7] Y. P. Li, Y. Qin, X. Chen, and W. Li, "Exploring the functional brain network of Alzheimer's disease: Based on the computational experiment," *PLoS ONE*, vol. 8, no. 9, p. e73186, 2013.

[8] T. Speed, "A correlation for the 21st century," *Science*, vol. 334, pp. 1502–1503, Dec. 2011.

[9] J. Hardin, A. Mitani, L. Hicks, and B. Vankoten, "A robust measure of correlation between two genes on a microarray," *BMC Bioinf.*, vol. 8, p. 220, Jun. 2006.

[10] J. Zhang *et al.*, "Mapping the small-world properties of brain networks in deception with functional near-infrared spectroscopy," *Sci. Rep.*, vol. 6, Apr. 2016, Art. no. 25297.

[11] M. S. Srivastava and G. C. Lee, "On the choice of transformations of the correlation coefficient with or without an outlier," *Commun. Statist.-Theory Methods*, vol. 12, no. 21, pp. 2533–2547, 2010.

[12] M. Chavez, M. Valencia, V. Navarro, V. Latora, and J. Martinerie, "Functional modularity of background activities in normal and epileptic brain networks," *Phys. Rev. Lett.*, vol. 104, no. 11, 2010, Art. no. 118701.

[13] J. Gross, J. Kujala, M. Hämäläinen, L. Timmermann, A. Schnitzler, and R. Salmelin, "Dynamic imaging of coherent sources: Studying neural interactions in the human brain," *Proc. Nat. Acad. Sci. USA*, vol. 98, no. 2, pp. 694–699, 2001.

[14] A. C. Chen, "EEG default mode network in the human brain: Spectral field power, coherence topology, and current source imaging," in *Proc. Joint Meeting 6th Int. Symp. Noninvasive Funct. Source Imag. Brain Heart Int. Conf. Funct. Biomed. Imag.*, Hangzhou, China, 2007, pp. 215–218.

[15] X. Li, J. Zhuang, B. Hu, and S. Sun, "An EEG-based study on coherence and brain networks in mild depression cognitive process," in *Proc. IEEE Int. Conf. Bioinf. Biomed.*, Dec. 2017, pp. 1275–1282.

[16] Z. J. Wang, P. W.-H. Lee, and M. J. Mckeown, "A novel segmentation, mutual information network framework for EEG analysis of motor tasks," *Biomed. Eng. Online*, vol. 8, p. 9, May 2009.

[17] J. Rudas *et al.*, "A method for functional network connectivity using distance correlation," in *Proc. Eng. Med. Biol. Soc.*, 2014, pp. 2793–2796.

[18] L. Su, L. Wang, H. Shen, G. Feng, and D. Hu, "Discriminative analysis of non-linear brain connectivity in schizophrenia: An fMRI Study," *Frontiers Hum. Neurosci.*, vol. 7, p. 702, Oct. 2013.

[19] B. Cassidy, C. Rae, and V. Solo, "Brain activity: Connectivity, sparsity, and mutual information," *IEEE Trans. Med. Imag.*, vol. 34, no. 4, pp. 846–860, Apr. 2014.

[20] Z. Zhang, S. Sun, M. Yi, X. Wu, and Y. Ding, "MIC as an appropriate method to construct the brain functional network," *Biomed Res. Int.*, vol. 2015, Oct. 2015, Art. no. 825136.

[21] B. Chai, D. Walther, D. Beck, and L. Fei-Fei, "Exploring functional connectivities of the human brain using multivariate information analysis," in *Proc. Adv. Neural Inf. Process. Syst.*, vol. 22, 2009, pp. 270–278.

[22] J. Rudas *et al.*, "A method for functional network connectivity using distance correlation," in *Proc. Eng. Med. Biol. Soc.*, 2014, pp. 2793–2796.

[23] D. Reshef, Y. Reshef, M. Mitzenmacher, and P. Sabeti. (2013). "Equitability analysis of the maximal information coefficient, with comparisons." [Online]. Available: https://arxiv.org/abs/1301.6314

[24] D. N. Reshef *et al.*, "Detecting novel associations in large data sets," *Science*, vol. 334, pp. 1518–1524, Dec. 2011.

[25] D. N. Reshef, Y. A. Reshef, M. Mitzenmacher, and P. C. Sabeti, "Cleaning up the record on the maximal information coefficient and equitability," *Proc. Nat. Acad. Sci. USA*, vol. 111, no. 33, pp. E3362–E3363, 2014.

[26] Y. A. Reshef, D. N. Reshef, H. K. Finucane, P. C. Sabeti, and M. M. Mitzenmacher, "Measuring dependence powerfully and equitably," *J. Mach. Learn. Res.*, vol. 17, no. 1, pp. 7406–7468, 2015.

[27] Q. Tan, J. Jiang, and Y. Ding, "Model selection method based on maximal information coefficient of residuals," *Acta Math. Sci.*, vol. 34, pp. 579–592, Mar. 2014.

[28] C. E. Shannon, "A mathematical theory of communication," *ACM SIGMOBILE Mobile Comput. Commun. Rev.*, vol. 5, no. 1, pp. 3–55, 2001.
[29] L. Su, L. Wang, S. Hui, G. Feng, and D. Hu, "Discriminative analysis of non-linear brain connectivity in schizophrenia: An fMRI study," *Frontiers Hum. Neurosci.*, vol. 7, p. 702, Oct. 2013.
[30] N. K. Logothetis, J. Pauls, M. Augath, T. Trinath, and A. Oeltermann, "Neurophysiological investigation of the basis of the fMRI signal," *Nature*, vol. 412, pp. 150–157, Jul. 2001.
[31] J. S. Lewin, "Functional MRI: An introduction to methods," *J. Magn. Reson. Imag.*, vol. 17, no. 3, pp. 383–385, 2003.
[32] I. Bojak, T. F. Oostendorp, A. T. Reid, and R. Kötter, "Connecting mean field models of neural activity to EEG and fMRI data," *Brain Topogr.*, vol. 23, no. 2, pp. 139–149, 2010.
[33] S. Mantri, D. Patil, P. Agrawal, and V. Wadhai, "Non invasive EEG signal processing framework for real time depression analysis," in *Proc. SAI Intell. Syst. Conf.*, 2015, pp. 518–521.
[34] Z. A. A. Alyasseri, A. T. Khader, M. A. Al-Betar, J. P. Papa, and O. A. Alomari, "EEG-based person authentication using multi-objective flower pollination algorithm," in *Proc. IEEE Congr. Evol. Comput. (CEC)*, Jul. 2018, pp. 1–8.
[35] Z. A. A. Alyasseri, A. T. Khader, M. A. Al-Betar, J. P. Papa, and O. A. Alomari, "EEG feature extraction for person identification using wavelet decomposition and multi-objective flower pollination algorithm," *IEEE Access*, vol. 6, pp. 76007–76024, 2018.
[36] Z. Alyasseri, A. Khader, M. P. Al-Betar, J. Papa, O. A. Alomari, and S. N. Makhadmeh, "Classification of EEG mental tasks using multi-objective flower pollination algorithm for person identification," *Int. J. Integr. Eng.*, vol. 10, no. 7, 2018.
[37] S. N. Abdulkader, A. Atia, and M.-S. M. Mostafa, "Brain computer interfacing: Applications and challenges," *Egyptian Inform. J.*, vol. 16, pp. 213–230, Jul. 2015.
[38] Z. A. A. Alyasseri, A. T. Khader, M. A. Al-Betar, J. P. Papa, O. A. Alomari, and S. N. Makhadme, "An efficient optimization technique of eeg decomposition for user authentication system," in *Proc. 2nd Int. Conf. BioSignal Anal., Process. Syst. (ICBAPS)*, 2018, pp. 1–6.
[39] A. von Stein and J. Sarnthein, "Different frequencies for different scales of cortical integration: From local gamma to long range alpha/theta synchronization," *Int. J. Psychophysiol.*, vol. 38, no. 3, pp. 301–313, 2000.
[40] C. Babiloni *et al.*, "Hippocampal volume and cortical sources of EEG alpha rhythms in mild cognitive impairment and Alzheimer disease," *NeuroImage*, vol. 44, pp. 123–135, Jan. 2009.
[41] Y.-W. Shin, T. H. Ha, S. Y. Kim, and J. S. Kwon, "Association between EEG alpha power and visuospatial function in obsessive–compulsive disorder," *Psychiatry Clin. Neurosci.*, vol. 58, pp. 16–20, Feb. 2004.
[42] S. Achard and E. Bullmore, "Efficiency and cost of economical brain functional networks," *PLoS Comput. Biol.*, vol. 3, no. 2, p. e17, 2007.
[43] Y. He *et al.*, "Impaired small-world efficiency in structural cortical networks in multiple sclerosis associated with white matter lesion load," *Brain*, vol. 132, pp. 3366–3379, Dec. 2009.
[44] Y. Tian and D. Yao, "Why do we need to use a zero reference? Reference influences on the ERPs of audiovisual effects," *Psychophysiology*, vol. 50, pp. 1282–1290, Dec. 2013.
[45] D. Yao, "A method to standardize a reference of scalp EEG recordings to a point at infinity," *Physiol. Meas.*, vol. 22, no. 4, pp. 693–711, 2001.
[46] A. Belouchrani, K. Abed-Meraim, J. F. Cardoso, and E. Moulines, "A blind source separation technique using second-order statistics," *IEEE Trans. Signal Process.*, vol. 45, no. 2, pp. 434–444, 2002.
[47] P. J. Benesty, J. Chen, Y. Huang, and I. Cohen, "Pearson correlation coefficient," in *Noise Reduction in Speech Processing*. Berlin, Germany: Springer, 2009.
[48] P. Sedgwick, "Spearman's rank correlation coefficient," *BMJ*, vol. 349, p. g7327, Nov. 2014.
[49] J. Wang, X. Wang, M. Xia, X. Liao, A. Evans, and Y. He, "GRETNA: A graph theoretical network analysis toolbox for imaging connectomics," *Frontiers Hum. Neurosci.*, vol. 9, p. 386, Jun. 2015.
[50] J.-R. Ding *et al.*, "Topological fractionation of resting-state networks," *PLoS ONE*, vol. 6, no. 10, p. e26596, 2011.
[51] M. Rubinov and O. Sporns, "Complex network measures of brain connectivity: Uses and interpretations," *NeuroImage*, vol. 52, no. 3, pp. 1059–1069, 2010.
[52] D. J. Watts and S. H. Strogatz, "Collective dynamics of 'small-world' networks," *Nature*, vol. 393, pp. 440–442, Jun. 1998.
[53] M. D. Humphries, K. Gurney, and T. J. Prescott, "The brainstem reticular formation is a small-world, not scale-free, network," *Proc. Roy. Soc. B, Biol. Sci.*, vol. 273, no. 1585, pp. 503–511, 2006.
[54] S. Maslov and K. Sneppen, "Specificity and stability in topology of protein networks," *Science*, vol. 296, no. 5569, pp. 910–913, 2002.
[55] H. M. Liu, N. Rao, D. Yang, L. Yang, Y. Li, and F. Ou , "A novel method for identifying SNP disease association based on maximal information coefficient," *Genet. Mol. Res.*, vol. 13, no. 4, pp. 10863–10877, 2014.
[56] J. N. Poynter *et al.*, "Cross platform analysis of methylation, miRNA and stem cell gene expression data in germ cell tumors highlights characteristic differences by tumor histology," *BMC Cancer*, vol. 15, p. 769, Oct. 2015.
[57] N. Langer, C. C. von Bastian, H. Wirz, K. Oberauer, and L. Jäncke, "The effects of working memory training on functional brain network efficiency," *Cortex*, vol. 49, p. 2424, Oct. 2013.
[58] J. J. Foxe and A. C. Snyder, "The role of alpha-band brain oscillations as a sensory suppression mechanism during selective attention," *Frontiers Psychol.*, vol. 2, p. 154, Jul. 2011.
[59] S. Palva and J. M. Palva, "Functional roles of alpha-band phase synchronization in local and large-scale cortical networks," *Frontiers Psychol.*, vol. 2, p. 204, Sep. 2011.
[60] W. J. Freeman and L. J. Rogers, "Fine temporal resolution of analytic phase reveals episodic synchronization by state transitions in gamma EEGs," *J. Neurophysiol.*, vol. 87, pp. 937–945, Feb. 2002.

YIN TIAN received the Ph.D. degree in biomedical engineering from the School of Life Science and Technology, University of Electronic Science and Technology of China, in 2009. She is currently a Professor with the Bio-Information College, Chongqing University of Posts and Telecommunications. Her research interests include cognitive neuroscience, EEG/fMRI data processing, machine learning, brain network technology, and brain–computer interface.

HUILING ZHANG received the bachelor's degree in biomedical engineering from the Bio-Information College, Chongqing University of Posts and Telecommunications, in 2016, where she is currently a Graduate Student. Her research interests include biomedical signal processing, working memory, emotional recognition, machine learning, and brain–computer interface.

PEIYANG LI received the Ph.D. degree in biomedical engineering from the University of Electronic Science and Technology of China, Chengdu, Sichuan, China, in 2018. He is currently with the Chongqing University of Posts and Telecommunications, Chongqing, China. His research interests include brain–computer interaction, convex optimization, machine learning, and pattern recognition.

YANG LI received the master's degree in electronics and communication engineering from the Information Science and Technology College, Chengdu University of Technology, in 2017. He is currently pursuing the Ph.D. degree with the Chongqing University of Posts and Telecommunications. His research interests include signal processing, machine learning, and brain–computer interface.